Effects of Composition of Oligo(ethylene glycol)-Based Mixed Monolayers on Peptide Grafting and Human Immunoglobulin Detection

Nafisa Islam,[†] Patrick V. Gurgel,[†] Orlando J. Rojas,[†,‡] and Ruben G. Carbonell*[,†,§]

[†]Department of Chemical and Biomolecular Engineering, North Carolina State University, Raleigh, North Carolina 27695, United States

[‡]School of Chemical Technology, Department of Forest Products Technology, Aalto University, P.O. Box 16300, 00076 Aalto, Finland

[§]Biomanufacturing Training and Education (BTEC), North Carolina State University, Raleigh, North Carolina 27695, United States

S *Supporting Information*

ABSTRACT: Alkanethiols carrying ethylene glycol units (EG$_n$, n = 3 or 6) with amine termini (EG$_3$NH$_2$ or EG$_6$NH$_2$) were coadsorbed with a "diluent", hydroxyl-terminated alkanethiol (EG$_3$OH), to form mixed self-assembled monolayers (SAMs). The mixed SAMs were characterized, and hexameric peptide ligand His-Trp-Arg-Gly-Trp-Val (HWRGWV), which shows affinity binding toward the Fc (constant fragment) of human immunoglobulin (IgG), was grafted onto different dilutions of EG$_6$NH$_2$−EG$_3$OH mixed SAMs for preparation of IgG detection surfaces. The specificity toward IgG was optimal for peptides grafted on SAMs prepared from 10% EG$_6$NH$_2$ precursor solution, even though this surface did not have the highest number of peptides per unit area. Surface plasmon resonance (SPR) experiments showed that IgG bound to the peptides on the mixed SAM with a dissociation constant K_d of 9.33 × 10^{-7}, maximum binding capacity Q_m of 3.177 mg m^{-2}, and adsorption rate constant k_a of 1.99 m^3 mol^{-1} s^{-1}. IgG binding from complex mixtures of Chinese Hamster Ovary supernatant (CHO) was investigated on peptides grafted to mixed and pure SAMs. Regeneration of the surfaces was achieved by treatment with 10% acetonitrile in 0.1 M NaOH solution. Overall, the use of peptides grafted on mixed SAMs improved the effectiveness of detection and had an impact on specificity and regeneration of biosensors.

IgG Adsorption on Peptide-Mixed SAM
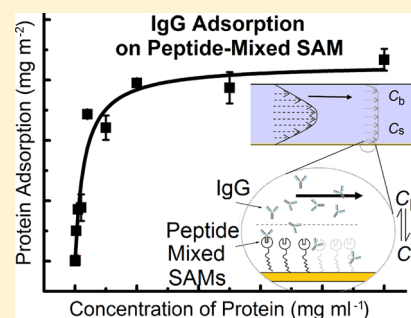
1. INTRODUCTION

The interface between the ligand and the transducer surface of a biosensor plays an important role in its performance. The incorporation of advanced materials for enhanced biocompatibility, improved biorecognition, decreased biofouling, and reduced nonspecific binding are active fields of research.[1] The optimal surface must be suitable for binding of ligands effectively and also must provide maximal specific recognition and minimal nonspecific binding. Self-assembled monolayers (SAMs) of alkanethiols are easily prepared, form well-defined structures, and are stable under biological conditions over extended periods of time,[2] making them suitable as an interface layer for biosensor applications. SAMs also provide the option of various covalently reacting termini for further modification.[3,4] Mixed SAMs have been used for enhanced binding as well as antibiofouling properties.[5,6] This study investigates the properties of mixed SAMs with either HS−(CH$_2$)$_{11}$−(CH$_2$CH$_2$O)$_3$−NH$_2$ (EG$_3$NH$_2$) or HS−(CH$_2$)$_{11}$−(CH$_2$CH$_2$O)$_6$−NH$_2$ (EG$_6$NH$_2$) diluted with HS−(CH$_2$)$_{11}$−(CH$_2$CH$_2$O)$_3$−OH (EG$_3$OH) and also explores their applicability for grafting hexameric peptide His-Trp-Arg-Gly-Trp-Val (HWRGWV) for binding of human immunoglobulin G (IgG). After HWRGWV grafting via the C-termini onto the EG$_6$NH$_2$ groups on the mixed SAMs, protein binding studies were carried out using surface plasmon resonance (SPR).

The common approach for preparation of mixed SAMs is to deposit two different alkanethiols simultaneously on a gold surface, where one thiol molecule carries a functional group that is capable of covalently binding the biological receptors and a second thiol may bear a functional group capable of reducing nonspecific adsorption.[6−10] In the design of biosensors, oligo(ethylene glycol) (OEG)-based SAMs have been used, to inculcate the hydrophilicity and bioresistance of the ethylene glycol (EG) units without having bulky/thick polymer layers. Even though fundamental studies involving OEG-based monolayers have been reported as early as 1991 by Prime and Whitesides,[11] related applications only began in the past decade. Alkanethiols with terminal carboxylate (−COOH) groups have been widely used in pure or mixed monolayers, and OEG-based alkylthiolates (SH−(CH$_2$)$_m$−EG$_n$COOH) have been recently characterized for biosensing purposes.[12−14]

Mixed SAMs based on linear alkanethiols with small molecular

variations in termini have been studied for biosensing and other applications.[15−18] Recently, studies have been carried out with mixed OEG-based alkanethiol monolayers.[2,8,13,19−21] The structure and properties of the mixed monolayers have an effect on the ligand immobilization and, in turn, on subsequent sensing properties. Properties of sets of mixed monolayers will not be necessarily similar when the terminal functional groups are changed.[22] Hence there is a need to characterize the mixed monolayers. To the best of our knowledge, EG_nNH_2 (n = 3 or 6) mixed with EG_3OH alkanethiols have not been utilized for biosensing purposes.

Quantification of the surface density of reactive termini and of the ligands grafted on the mixed SAMs is necessary because of their influence on the effectiveness of biosensing. Techniques like X-ray photoelectron spectroscopy (XPS)[23] and ellipsometry[12,24] can be used for quantification. SPR allows real-time analysis of interactions between analytes in solution and surface-immobilized ligands[25−27] by generating a continuous experimental readout of complex formation and dissociation. Affinity data help to understand the strength of interaction and binding behavior between biomolecules in question, at equilibrium, while knowledge of rate constants k_a and k_d reveals kinetic information pertaining to the binding mechanism.

The application of short peptides is an alternative to protein-based biosensors due to the potentially lower costs of preparing large amounts of highly pure ligands and relative ease of modification for enhanced binding.[28] A hexamer peptide ligand, HWRGWV, identified from a one-bead−one-peptide combinatorial library was synthesized on chromatography resins and found to exhibit high affinity and specificity to the Fc fragment of IgG.[29] A chromatography resin with HWRGWV was able to purify human IgG from two different commercial CHO cell culture media with high levels of purity, and multiple cycles of regeneration of these resins have been demonstrated.[30,31] Peptide HWRGWV may be grafted onto a random copolymer layer rich in primary amines, and IgG binding has been successfully demonstrated on these diverse matrices using SPR and quartz crystal microgravimetry (QCM).[32] The success of IgG binding on the peptide layers on polymers has demonstrated that there is a potential for construction and application of a variety of peptide-based matrices for IgG separation. In this study, matrices for peptide grafting are the oligo(ethylene glycol)-based mixed SAMs.

The properties of the mixed SAMs have been determined in this study using X-ray photoelectron spectroscopy (XPS), time-of-flight secondary ion mass spectroscopy (ToF-SIMS), contact angle goniometry, and ellipsometry. ToF-SIMS was used to estimate the surface concentration of alkanethiols in the mixed SAMs, and ellipsometric measurements were used to quantify the number of reactive species and subsequently determine the extent of reaction of the amine moieties in the SAMs. Contact angle measurements were carried out to investigate the presence of phase-separated domains. The mixed SAMs were used for enhanced biosensing after grafting of active HWRGWV ligands. We compared the applicability of EG_6NH_2−EG_3OH SAMs for sensor preparation, and this set of mixed SAMs was chosen as the NH_2 moiety is hypothesized to have better access to the ligand due to the three additional ethylene glycol units of the active thiol.[33] SPR protein binding studies were carried out, and the optimal mixed SAM concentration was chosen for further performance analysis in IgG detection. Sensors with a base matrix of pure and mixed

monolayers were compared to study their behavior toward complex mixtures containing the analyte. Finally the regeneration potential of sensors based on pure and mixed SAMs carrying the grafted peptides was demonstrated.

2. EXPERIMENTAL SECTION

2.1. Materials. Bioresistant alkanethiols, (11-mercaptoundecyl)hexa(ethyleneglycol)ammonium-hydrochloride (EG_6NH_2), (11-mercaptoundecyl)tri(ethyleneglycol)-ammonium-hydrochloride (EG_3NH_2), and (11-mercaptoundecyl)tri(ethyleneglycol) (EG_3OH), were obtained from Prochimia Surfaces Inc. (Sopot, Poland). Ethanol (200 proof) was obtained from Pharmaco-AAPER (Charlotte, NC). N,N-Dimethylformamide (DMF, ACS reagent, 99.8%), anhydrous DMF, diisopropylethylamine (DIPEA), glacial acetic acid (ACS reagent 99.5%), bovine serum albumin (BSA, 98%), phosphate-buffered saline (pH 7.4, monobasic sodium phosphate, dibasic sodium phosphate, sodium chloride 0.138 M, potassium chloride 0.0027 M), and triethylene amine (TEA, ACS reagent 99%) were all obtained from Sigma-Aldrich (St. Louis, MO). 2-(1H-7-Azabenzotriazol-1-yl)-1,1,3,3-tetramethyl uronium hexafluorophosphate (HATU) was purchased from ChemPep Inc. (Wellington, FL). Human immunoglobulin G (IgG, 97% purity) was obtained from Equitech-Bio, Inc. (Kerrville, TX). Deionized water (resistivity >15 MΩ·cm) and Milli-Q water (MQ water, resistivity >18 MΩ·cm) were obtained by using a Millipore water purification system (Billerica, MA). Nitrogen gas was obtained from Airgas National Welders (Raleigh, NC). Acetylated-His-Trp-Arg-Gly-Trp-Val-OH was custom synthesized by Genscript Inc. (Piscataway, NJ) at >97% purity. Sodium hydroxide (NaOH) and sodium acetate (CH_3COONa) were obtained from Fisher Chemicals (Pittsburgh, PA). Chinese hamster ovary (CHO) cell culture supernatant mixtures were a gift from Biogen Idec Inc. (Morrisville, NC). Serum-free media CHO-S-SFM II (SFM II) was obtained from Life Technologies (Grand Island, NY).

2.2. Gold Slides and Sensors. For ellipsometric experiments glass slides (25 × 6.25 × 1 mm) coated with 100 nm of gold from EMF Corporation (Ithaca, NY) were used. The SPR experiments utilized glass sensor chips (12 × 20 × 0.5 mm) sputtered with a 50 nm gold layer on top of 2 nm of chromium from KSV Instruments OY (Helsinki, Finland), while other characterization experiments required silicon wafers coated with 100 nm over a 5 nm Ti adhesion layer from Platypus Technologies (Madison, WI), cut into approximately 1 cm × 1 cm pieces. These were cleaned prior to use by soaking in Piranha solution (98% H_2SO_4 and 30% H_2O_2 at 7:3 v/v) for 15−20 min, followed by profuse rinsing in MQ water, further rinsing in 200 proof ethanol, and finally drying under a stream of nitrogen gas. The surfaces were immersed in ethanol for no more than 30 min before being added to freshly prepared solutions for further modification. (*Warning: Piranha solution reacts violently with organic materials and should be handled with extreme caution.*)

2.3. Self-Assembled Monolayer (SAM) Formation. Alkanethiol EG_6NH_2 or EG_3NH_2 mixed with EG_3OH thiol (total concentration, 1 mM) were dissolved in 200-proof ethanol. Gold slides or sensors were left in the precursor thiol solutions under nitrogen gas away from light. Samples prepared for X-ray photoelectron spectroscopy (XPS) and time-of-flight secondary ionization mass spectra (ToF-SIMS) remained in thiol solutions for a period of 48 h to ensure complete and
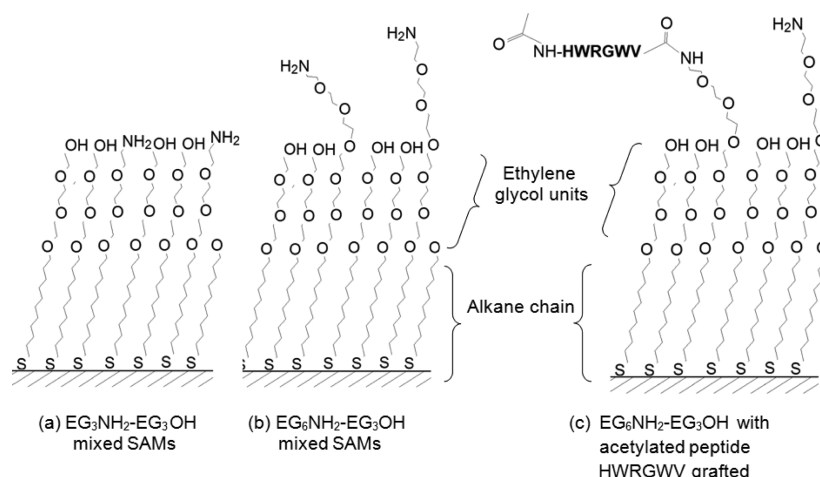
Figure 1. Schematic diagram, not to scale, showing the two systems of mixed alkanethiolates being studied, (a) $EG_3NH_2-EG_3OH$ and (b) $EG_6NH_2-EG_3OH$, and (c) acetylated peptide ligand HWRGWV attached via C-termini to NH_2 moieties on $EG_6NH_2-EG_3OH$.

uniform coverage. The sensors were removed and rinsed thoroughly with ethanol, followed by a 5 min sonication in ethanol, followed again by rinsing in ethanol. Finally the sensors were dried under a stream of nitrogen gas and immediately used for XPS or ToF-SIMs analysis. For ellipsometry and SPR experiments, and also for subsequent peptide grafting, the slides or sensors were immersed in thiol solutions dissolved in ethanol with 3% (v/v) TEA to ensure complete monolayers in a shorter time.[34] After 24 h, these surfaces were rinsed with ethanol followed by soaking in a 10% (v/v) acetic acid aqueous solution. The surfaces were then sonicated in 10% acetic acid for 2 min, followed by rinsing with ethanol and sonication in ethanol. The surfaces were finally rinsed with ethanol and dried under a stream of nitrogen gas. A schematic illustration of mixed SAMs $EG_3NH_2-EG_3OH$ and $EG_6NH_2-EG_3OH$ is shown in Figure 1(a) and (b), respectively. The peptide grafted on the $EG_6NH_2-EG_3OH$ mixed SAM is depicted in Figure 1(c). The mixed SAMs tested consisted of EG_nNH_2 concentrations in the range of 0−100% of precursor solution concentration, unless otherwise mentioned.

2.4. Grafting of Peptide. Peptide acetylated HWRGWV was grafted onto the −NH_2 of the $EG_6NH_2-EG_3OH$ mixed SAM (Figure 1(c)) by using chemistries similar to those previously reported for chromatographic resins.[31] Briefly, HWRGWV was coupled by immersing the slides or sensors in anhydrous DMF containing HWRGWV, HATU, and DIPEA at 5, 10, and 20 mM, respectively. The slides/sensors and the appropriate peptide solutions were purged with a stream of nitrogen gas, and the container was sealed to avoid exposure to atmospheric moisture. The system was left on a shaker at 250 rpm overnight at room temperature. After completion of the peptide grafting reaction, the slides/sensors were rinsed with ACS-grade DMF followed by sonication in DMF for 5 min. Finally, the sensors were rinsed again in DMF after which they were dried under a stream of nitrogen gas.

2.5. X-ray Photoelectron Spectroscopy (XPS) of $EG_3NH_2-EG_3OH$ Mixed SAM. The surface chemical compositions of the dried samples of $EG_3NH_2-EG_3OH$ mixed SAM were determined via XPS. The measurements were performed using an AXIS 165 electron spectrometer (Kratos Analytical, Manchester, UK) and a monochromatic Al Kα X-ray irradiation at 100 W (ca. 1 mm² and <10 nm analysis

area and depth, respectively). High-resolution spectra of carbon (C 1s) and oxygen (O 1s) were collected, and elemental wide region data for nitrogen (N 1s) and sulfur (S 2p) were collected. All spectra were recorded at several different points on each sample. Prior to the XPS, the samples were kept under vacuum in a chamber overnight, and an in situ reference of pure cellulose[35] was used to verify satisfactory experimental vacuum conditions during the analysis of each sample batch. No sample degradation (due to ultrahigh vacuum or X-rays) was observed during the measurements.

2.6. Time-of-Flight Secondary Ion Mass Spectroscopy (ToF-SIMS) of $EG_3NH_2-EG_3OH$ and $EG_6NH_2-EG_3OH$ Mixed SAMs. The modified gold slides with mixed SAMs of $EG_3NH_2-EG_3OH$ and $EG_6NH_2-EG_3OH$ were analyzed using an ION-TOF SIMS 5 instrument (ION-TOF GmbH, Münster, Germany). A static model was chosen, and the equipment was operated at a pressure below 1×10^{-8} mbar. A Bi+ source operating at 25 keV was used. The data points were collected at three points each on multiple samples at various concentrations of monolayers. Various authors studying SAMs using ToF-SIMS or other MS methods have suggested use of negative spectra molecular fragment peaks characteristic to the SAM[36] and negative spectra standards (typically Au cluster ion peaks).[37−39] The N-containing molecular fragments from positive spectra are usually chosen when analyzing peptide or protein molecules.[40] Thus, we present our results from characteristic N cluster ion peaks that are characteristic of the NH_2-containing thiol, and we have chosen the negative spectra Au cluster ion peaks to normalize these peak areas. The mass scale for negative secondary ions was calibrated primarily using peaks originating from C_2H^-, CH_2^-, and Au_2S^-. Ion peaks which would be characteristic for NH_2-terminating thiols were chosen, and their corrected peak areas were calculated using ION-TOF software. To represent the total amount of NH_2 thiol on the mixed monolayer surface, the following expression was used to normalize the areas[41]

$$\frac{\sum \text{Area of characteristic molecular peaks for } NH_2-\text{thiol}}{\sum \text{Area of normalization molecular peaks of Au}}$$
$$= \frac{\text{Peak Area}_{CN^-} + \text{Peak Area}_{CNO^-}}{\text{Peak Area}_{Au^-} + \text{Peak Area}_{Au_2^-} + \text{Peak Area}_{Au_3^-} + \text{Peak Area}_{Au_4^-}}$$

$$(1)$$

2.7. Contact Angle Goniometry of the EG$_6$NH$_2$–EG$_3$OH SAM. Water contact angles on the prepared mixed SAMs of EG$_6$NH$_2$–EG$_3$OH were measured using a model 200 Standard Contact Angle Goniometer with Dropimage standard software (Ramé-Hart, Mountain Lakes, NJ). Advancing and receding contact angles were measured using the sessile drop method.

2.8. Surface Density of the EG$_6$NH$_2$–EG$_3$OH SAM and Grafted Ligands by Ellipsometry. The layer thicknesses of the EG$_6$NH$_2$–EG$_3$OH SAM on the gold slides, before and after peptide grafting, were measured by ellipsometry using an Alpha-SE spectroscopic ellipsometer (J.A.Woollam, Lincoln, NE) at an angle of incidence $\Phi = 70°$ and a wavelength range of 380−900 nm. Five points were measured on multiple slides, and the average thickness was noted with refractive index, n, fixed at 1.45. The measured ellipsometric layer thicknesses were converted into the number of molecules per unit area by using eq 2 as an approximation.[42]

$$\Gamma = \frac{\rho d N_A 10^{-22}}{M_w} \tag{2}$$

where Γ is the surface density in molecules nm^{-2}; d is the ellipsometric thickness in Å; ρ is the specific gravity of the species in g cm^{-3}; N_A is the Avogadro's constant; and M_w is the molecular weight of the species. The maximum theoretical diameter and theoretical area occupied by a peptide were found using the visualization and measurement tools of a space filling model software, PYMOL (Delano Scientific Inc.), assuming hexagonal packing of peptides.

2.9. Surface Plasmon Resonance (SPR) Experiments and Calculation of Equilibrium and Kinetic Constants. A KSV SPR 200 instrument (BioNavis Instruments, Helsinki, Finland) was used to detect variations in the refractive index at the interface of the sensor, and the experimental details were followed as described in the Supporting Information. Briefly, buffer solution flowed over the gold surface with attached ligands, in the fluidic system. The sample was injected by means of two injector valves, with 200 μL in volume each, into the buffer flow, and this flowed over the gold surface of the glass slide. All experiments were carried out at 0.5 °C below room temperature to minimize the possibility of introducing gas bubbles during measurements. All buffers and solutions were degassed before injection or before flowing into the SPR system.

SPR Calibration. The SPR instrument was calibrated to generate a standard curve relating the SPR response to changes in refractive index (RI), details of which can be found in the Supporting Information, Section S1. The change in RI in experiments of protein binding was converted to adsorbed mass of a biomolecule by using the model of Jung et al.[25]

Protein Binding. SPR sensors with peptide grafted onto EG$_6$NH$_2$–EG$_3$OH mixed SAMs were used for protein binding experiments. Solutions of analyte human immunoglobulin G (IgG) were prepared in PBS solution (pH 7.4, with 1 M NaCl added to buffer) at different concentrations. Bovine serum albumin (BSA) solutions at different concentrations in the same buffer were used to quantify nonspecific adsorption. The baseline in SPR was obtained by maintaining 10 μL min^{-1} of PBS. Protein solutions were injected via 200 μL sample loops at a constant flow rate of 10 μL min^{-1}. The SPR was switched back to buffer solution at the end of the injection time. The binding experiments were carried out on newly prepared sensors each time.

Calculation of the Equilibrium Constant of IgG Binding. The maximum net change of signal that occurred after IgG injection at different concentrations was recorded during the SPR experiments. The intensity changes were converted into units of adsorbed mass per unit area. Protein IgG isotherms were plotted versus the bulk IgG concentration and fitted to a simple Langmuir model that used the adsorbed mass Q (mg m^{-2}) and the bulk concentration C (M) as variables

$$Q = \frac{Q_m C}{K_d + C} \tag{3}$$

Here, K_d is the equilibrium dissociation constant (M), and Q_m is the maximum binding capacity (mg m^{-2}).

Determination of Kinetic Constants of IgG Binding. It can be assumed that the IgG and the ligand Lg on the surface (peptide) bind reversibly forming a complex IgG−Lg as indicated in the expression[43]

$$\text{IgG} + \text{Lg} \underset{k_d}{\overset{k_a}{\rightleftharpoons}} \text{IgG−Lg} \tag{4}$$

The rate of adsorption can be assumed to be a second-order reaction with a rate constant k_a, and the desorption step can be assumed to be a first-order reaction proportional to the concentration of the IgG−Lg complex on the surface with a desorption rate constant k_d

$$\frac{d[\text{IgG−Lg}]}{dt} = k_a[\text{IgG}][\text{Lg}] - k_d[\text{IgG−Lg}] \tag{5}$$

The antibody concentration [IgG] in eq 5 is the concentration of antibody in the liquid phase directly adjacent to the interface. Because of diffusional limitations, the concentration at the interface at a given time might be different from the concentration of antibody in the bulk solution. For simplicity, the concentration of IgG at the surface is labeled C_s, and the analyte concentration of the bulk solution is labeled C_b. The flux of solute (mole/area/time) from the bulk to the interface is governed by an average mass transfer coefficient k_m whose magnitude depends on known values of the superficial velocity, the gap width above the surface, and the diffusion coefficient of the antibody. The flux can also be expressed in terms of the concentration difference between the bulk and at the interface as is represented in eq 7. Since all molecules diffusing to the interface are assumed to bind, the mass transfer flux is equal at all times to the flux due to adsorption. The total ligand concentration on the surface is constant and equal to the sum of bound and unbound (free) ligand, i.e., [IgG−Lg] + [Lg]. The SPR response R (arbitrary units) can be assumed to be proportional to the amount of bound [IgG−Lg]; the maximum response due to analyte binding, R_{max}, is proportional to the total ligand concentration; and $(R_{max} - R)$ is equivalent to the free ligand concentration. If C_s is the IgG concentration at the interface, eq 5 can be rewritten in the form

$$\frac{dR}{dt} = k_a C_s (R_{max} - R) - k_d R \tag{6}$$

The rate of change of the ligand−analyte complex at the interface is equal to the flux of antibody to the interface due to mass transfer
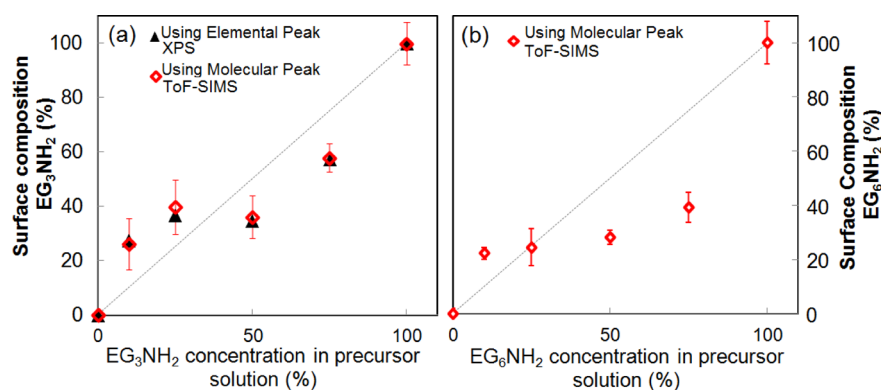
Figure 2. (a) Experimental results for EG_3NH_2–EG_3OH mixed SAMs with XPS (black profile) and ToF-SIMS (red profile) showing a good correspondence of elemental nitrogen (N 1s) and molecular N-containing peak data, respectively. (b) Experimental results of EG_6NH_2–EG_3OH mixed SAMs from ToF-SIMS results (red profile). (Both XPS data and ToF-SIMS peak data are expressed as a percentage of the respective highest N-containing sample, i.e., SAMs formed from 100% EG_nNH_2 precursor solution. The dotted lines are plotted as hypothetical reference points where the EG_nNH_2 surface composition equals the concentration in precursor solution.)

$$\frac{dR}{dt} = k_m(C_b - C_s) \qquad (7)$$

The isotherm parameters Q_m (directly proportional to R_{max}) and K_d can be obtained from equilibrium adsorption measurements. The rate constants for adsorption and desorption are related to the equilibrium dissociation constant by the expression $K_d = k_d/k_a$. The details of calculation of k_m can be found in the Supporting Information, Section S2. Dynamic adsorption data of signal R as a function of time can be analyzed using eqs 6 and 7 by finding the best value of the parameter k_a that fits the data. For further evaluation of the binding process and to determine whether binding is mass transport limited or rate limited the following analysis was carried out analyzing the C_s/C_b profile, and details of this analysis can be found in the Supporting Information, Section S2. Briefly, when $k_m \gg k_a$, binding is reaction rate limited, and $C_s/C_b \to 1$ from the onset of binding. Conversely when $k_a \gg k_m$ binding is mass transport limited, and $C_s/C_b < 1$ at time $t \to 0$.

Complex Mixture Experiment. Chinese hamster ovary (CHO) cell culture supernatant mixtures were diluted with buffer (PBS pH 7.4, with 1 N NaCl added to buffer) or with serum-free media (SFM II) and passed over peptide grafted onto 100% EG_6NH_2 and mixed SAMs formed from 10% EG_6NH_2 precursor solution. The net difference in SPR signal before and after the CHO dilution injection event was observed. This can be converted to find the quantity of protein adsorbed from the CHO dilution. These values help calculate the percentage deviation from the theoretical SPR signal that would have been generated if the IgG had been detected from pure (buffer) solutions of IgG. The theoretical values of the signal are calculated using eq 3 with the appropriate concentration of IgG (in the CHO dilution) as an input value for C. Knowing the constants Q_m and K_d, Q can be calculated, against which the percentage deviation from the theoretical can be calculated.

Regeneration Experiments. SPR sensors with peptide grafted onto 100% EG_6NH_2 and mixed SAMs formed from 10% EG_6NH_2 precursor solution were used for regeneration experiments. A 0.5 mg mL^{-1} solution of IgG in PBS solution (pH 7.4, with no added NaCl) was injected onto 100% EG_6NH_2–peptide surfaces. Before measurement, SPR baselines were obtained by maintaining a 20 μL min^{-1} flow of PBS.

Following the IgG binding step and a wash with buffer, injections of various regeneration solutions were carried out. The regeneration solutions tested were acetate buffer (0.1 M, pH 4.5), sodium hydroxide (0.1 M), and sodium hydroxide (0.1 M) mixed with 10% acetonitrile. Among these solutions the optimum regeneration solution was used in regeneration experiments on sensors with peptides grafted on mixed SAMs formed from 10% EG_6NH_2 precursor solutions. These experiments were done with the same protocol as on pure monolayer–peptide surfaces. IgG in PBS was introduced at 20 μL min^{-1} and allowed to bind for 7 min, followed by buffer injection for 5 min. After this, the regeneration solution was injected twice for 4 min each with 4 min of buffer flow between injections. IgG was injected again, and the cycle was repeated to test the regeneration capacity of the system.

3. RESULTS AND DISCUSSION

3.1. Estimation of Surface Composition of Mixed SAMs. In X-ray photoelectron spectroscopy (XPS) measurements, the nitrogen (N 1s) signal is used as a fingerprint for the amine-containing molecules present in the mixed SAM.[44] The average N content on the mixed SAM surface (filled triangles in Figure 2(a)) was expressed as a percentage of the N content of pure amine-terminated SAM, formed from 100% EG_3NH_2 precursor solution. The detailed results showing the elemental percentages of N, O, and S are reported in the Supporting Information (Table S1) together with a plot of the calculated N/S and N/O ratios for the samples formed from EG_3NH_2–EG_3OH mixtures (Figure S2, Supporting Information). Here, the N/S and N/O data are useful since they normalize the contribution of N 1s photoelectrons with respect to that of O 1s and S 2p in a given sample (internal calibration).

Mass spectrometry (MS) methods are usually employed for qualitative analysis to detect the presence of molecules according to the molecular weights and fractions of molecular ions and ion fragments. MS can be used for semiquantitative determination of the surface density of mixed monolayers, provided the characteristic peaks of the component molecules of the mixed systems are properly identified at a unique m/z ratio.[45] To use the results of time-of-flight secondary ion mass spectrometry (ToF-SIMS) for molecular peaks for calculating surface concentration, certain conditions must be fulfilled; for example, a series of closely chemically related samples should

be measured under the same experimental conditions.[46] In general, ToF-SIMS is not commonly used for determining quantitatively the molecular surface concentration on a surface.[38] However, characterization of monolayers with XPS or infrared spectroscopy can be complemented by other methods such as ToF-SIMS[26] and ellipsometry.[47−50] The EG_3NH_2 relative concentration calculated from ToF-SIMS peak areas for samples from alkanethiols with different percentages of EG_3NH_2 thiol is shown in Figure 2(a).

The XPS elemental N peak values and ToF-SIMS molecular fragment peak data for N-containing fragments are expressed as percentages of the respective highest N-containing sample, i.e., samples from 100% EG_3NH_2 precursor solution. As seen in Figure 2(a), there was agreement between XPS and ToF-SIMS results. The trends in the XPS N/O and N/S surface composition ratio as a function of EG_3NH_2 solution concentration (Table S1 and Figure S2, Supporting Information) not only confirm the presence of $EG_3NH_2−EG_3OH$ mixtures in the SAMs but further agree with the observed nonlinear trend for the surface compositions of $EG_3NH_2−EG_3OH$ with respect to the precursor solution concentrations. Also, there is shift in preferential adsorption of one thiol component over the other, after a certain concentration of SAMs is reached, and the shift is seen in both XPS and ToF-SIMs results for this mixed SAM.

We are very interested in the behavior of a similar but not exactly identical pair of alkanethiols, for purposes of fabricating and characterizing sensing surfaces for effective detection of IgG. The alkanethiol pair is $EG_6NH_2−EG_3OH$, and henceforth we focus our analysis toward properties of mixed monolayers formed from precursor solutions of $EG_6NH_2−EG_3OH$ SAMs. The surface concentrations were estimated using ToF-SIMS, and this method was suited for semiquantitative characterization. We applied the same method of analysis based on the molecular peaks as was done for $EG_3NH_2−EG_3OH$. Similar to the results for a $EG_3NH_2−EG_3OH$ mixed SAM, the surface compositions of $EG_6NH_2−EG_3OH$ were not linearly related to the EG_nNH_2 concentration in the precursor solution. ToF-SIMS surface composition calculations in $EG_3NH_2−EG_3OH$ (Figure 2(a)) and $EG_6NH_2−EG_3OH$ (Figure 2(b)) show that there is a dominant tendency for EG_nNH_2 to adsorb from solution when the EG_nNH_2 precursor solution concentrations are below 45% and 25%, respectively. Such adsorption selectivity has been observed by other authors[51] who have attributed this behavior to the preferential adsorption from a polar solvent of the less polar thiol (EG_nNH_2 in our case). Kang et al.[52] have also observed the shift in preferential adsorption when coadsorbing two thiols having polar end groups from a polar solvent. We observe a similar trend in the change of preferential adsorption of EG_3NH_2 or EG_6NH_2 which occurs at a particular but unique precursor solution dilution.

Kang et al. have postulated three governing factors that influence the partitioning in the adsorption of binary mixtures of thiols: the relative adsorption and desorption kinetics of the thiols, the polarity of the individual components, and the final electronic structure of the resulting SAM. Below a certain concentration of the EG_nNH_2, the preferential adsorption of EG_nNH_2 occurs because the EG_3OH has higher polarity and higher hydrogen bonding probability with the ethanol solvent, producing less extensive adsorption compared to that of NH_2-terminating molecules. Also preferential desorption of EG_3OH occurs contributing to the preferential adsorption of NH_2-terminated molecules. Kang explains that if the SAM

components are both polar molecules but with different polarities and are coadsorbing from a polar solvent the SAMs will have reduced stability due to different polarities. However, if coadsorption is from the polar solvent, the SAMs will be stabilized by interactions with polar solvent molecules. In the case of $EG_3NH_2−EG_3OH$, beyond 45% EG_3NH_2 precursor solution concentration, the concentration of EG_3NH_2 on the surface increases so much that intermolecular repulsion within the polar molecules in the SAM balances the adsorption−desorption kinetics effects. Adsorbed EG_3NH_2 desorbs into the solution at a faster rate compared to EG_3OH. At lower concentrations of EG_3NH_2, the SAM EG_3NH_2 does not desorb at a fast rate because of the stabilizing interactions of the polar solvent molecules on the molecules in the formed SAMs. It has been seen that the change of preferential adsorption of component thiols is absent in the case of coadsorption of nonpolar thiols or when coadsorbing from nonpolar solvents.[52] Thus, at higher EG_nNH_2 concentrations of the precursor solutions monolayers display apparent higher rates of preferential desorption of the NH_2-terminated thiol. For $EG_6NH_2−EG_3OH$ systems, the formed SAMs are even less stable compared to the $EG_3NH_2−EG_3OH$ because of the different lengths of component SAMs. The number of EG_6NH_2 molecules required to offset the stabilizing effects of the polar solvent is lower. The change in preferential adsorption is seen at 25% precursor solution concentration. Evidence of preferential adsorption of EG_nNH_2, especially at lower precursor solution concentrations, is seen in results of subsequent sections as well.

3.2. Characterization of $EG_6NH_2−EG_3OH$ Using Contact Angle Goniometry.
In our mixed SAMs an almost linear decrease of advancing contact angles, from $50 \pm 5°$ (EG_6NH_2) to $35 \pm 5°$ (EG_3OH), was observed (Figure 3). The contact
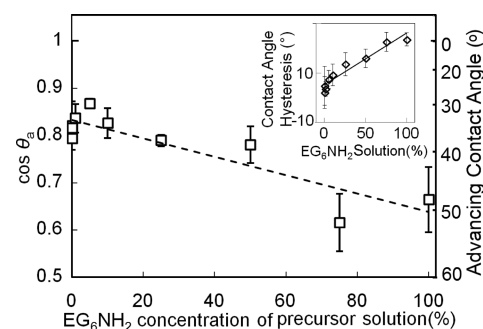

Figure 3. Advancing contact angle (right axis) and cosine of advancing contact angle (left axis) for $EG_6NH_2−EG_3OH$ mixed monolayer systems against concentration of EG_6NH_2 in the precursor thiol solutions. (Inset) Contact angle hysteresis plotted against concentrations of EG_6NH_2 in the precursor thiol solutions.

angle values were in agreement with those measured for diethyleneglycol-based mixed SAMs with amine- and hydroxyl-terminated thiols described by Chirakul et al.[24] However the $EG_6NH_2−EG_3OH$ mixed SAMs formed from 25% EG_6NH_2 precursor solutions or below show contact angles clustered closer to 50°, which again shows the preferential adsorption tendencies of one thiol over the other up to a certain concentration. Amine-terminated SAMs without OEG groups investigated by other authors[53,54] had contact angle values of $\geq 50°$ which indicates that the OEG groups in our systems increased the hydrophilicty of the SAM.

Table 1. Ellipsometric Lengths, Surface Densities of SAM Components and Grafted Peptides, and Corresponding Efficiencies of Peptide Grafting

EG$_6$NH$_2$ concentration in precursor solution (%)	thickness (Å)		surface density (molecules nm^{-2})		peptide grafting efficiency (%)
	mixed SAM	mixed SAM with grafted peptide ligand	EG$_6$NH$_2$ SAMs before peptide grafting	peptide	
1	16.5 ± 2.9	16.5 ± 1.5	2.68 ± 0.47	0.005	0.16 ± 0.06
5	21.2 ± 3.0	28.5 ± 2.6	2.26 ± 0.31	0.50 ± 0.28	22 ± 16
10	20.0 ± 1.3	31.1 ± 2.0	2.79 ± 0.18	0.77 ± 0.26	28 ± 11
25	19.7 ± 0.1	31.8 ± 1.9	2.72 ± 0.01	0.84 ± 0.20	31 ± 8
50	25.1 ± 2.1	32.0 ± 0.4	3.41 ± 0.29	0.48 ± 0.15	14 ± 5
100	25.4 ± 1.4	32.0 ± 0.02	2.66 ± 0.15	0.49 ± 0.01	18 ± 5

The water contact angle hysteresis was in general less than 20°, which is similar to that found for well-ordered SAMs of pure alkanethiolates on gold (Figure 3 (inset)). In our mixed monolayer systems the change in hysteresis from 0% EG$_6$NH$_2$ to 100% EG$_6$NH$_2$ SAMs was smooth and almost linear; sudden changes in hysteresis would have suggested formation of phase-separated domains or highly heterogeneous surfaces.[55,56]

The properties of mixed SAMs influence the analyte binding onto the biosensor surfaces which employ them as a linking layer between the ligand and transducer surface. Furthermore, the amount and spacing of ligands grafted onto the mixed SAM are also influenced by the surface composition and wettabilities of the SAM surfaces, which in turn will affect the sensitivity and specificity of biosensor surfaces. Thus characterizing the properties of mixed SAMs qualitatively and quantitatively can be vital for the development of improved biosensors.

3.3. Peptide Ligand Surface Density. In previous studies it has been suggested that by diluting the supporting SAMs one can control the amount of grafted ligands and decrease the number of reactive functional groups on biosensors, leading to an increase in accessibility of the analyte to the ligand, as well as decreasing the nonspecific adsorption by more bioresistant species available on the surface. These considerations are important when controlling analyte binding and in the development of biosensors with improved selectivities.[57,58]

The layer thicknesses can be used to quantify the amount of material on the surface by assuming the layer as having a constant refractive index.[27,59,60] Zhu et al.[61] calculated the lengths of SAMs formed by n-alkanethiols and OEG containing alkanethiols from ellipsometry measurements, assuming a value of 1.46 for the refractive index. Wang et al. chose 1.45 for organic layers, and 1.5 was chosen as the refractive index for protein-based layers.[59]

In our studies, for all ellipsometric measurements, the Cauchy model was chosen with fixed refractive index to determine the effective thickness of various layers for the sake of comparison of peptide layer surface density to SAM layer density. It was observed that when fitting the model with ellipsometric lengths and refractive indices of layers as unknown parameters SAM refractive indices between 1.45 and 1.5 would be obtained. It was also observed that changing the refractive index from $n = 1.45$ up to $n = 1.5$ did not change the ellipsometric lengths by more than 1 Å. Table 1 lists the ellipsometric thicknesses measured for the various mixed SAMs, before and after ligand attachment.

It is assumed that the chemical composition of the terminal group does not strongly affect the layer thickness of SAMs of the alkanethiols on gold, especially if the functional terminal groups have similar sizes. This applies to methyl- and amine-terminated alkanethiol, which have similar hydrodynamic radii.

However, the hydroxyl group is smaller than these two functional groups, and therefore the stated consideration may not apply.[9] The ellipsometric lengths of EG$_3$OH and EG$_3$NH$_2$ SAMs were 12 ± 1 and 18 ± 1 Å, respectively, which goes well with the above considerations. As a reference, the thickness for a similar OEG-based alkanethiol in Zhu's studies was 17 ± 1 Å. For pure EG$_6$NH$_2$ SAMs a thickness of 25 ± 1 Å was determined (compared with 24 ± 1 Å for similar OEG-based molecules reported by Zhu).

We have used the ToF-SIMS surface density approximations in conjunction with the ellipsometric lengths to estimate the exact numerical density of both alkanethiol molecules and subsequently of the peptides. The calculated density of EG$_6$NH$_2$ on the gold surface was a maximum for 50% EG$_6$NH$_2$ precursor solution.

The peptide surface densities were calculated from the change in ellipsometric lengths due to covalent grafting of peptides on the SAMs with varying EG$_6$NH$_2$ surface densities. The efficiency of peptide grafting was calculated as the ratio of the number of molecules of peptide to the number of NH$_2$ moieties available before grafting reaction. As is seen from the results, the molecular surface density ranges from 0 to 0.84 molecules nm^{-2} with the maximum occurring at the surface prepared from 25% EG$_6$NH$_2$ precursor solution. The efficiencies of peptide grafting on the SAMs show relatively higher values for surfaces prepared from between 10% and 25% EG$_6$NH$_2$ precursor solution. The relatively higher conversion for SAMs in this range of EG$_6$NH$_2$ precursor solution concentration may arise due to the optimal NH$_2$ spacing on the surface, and this has been investigated in a subsequent section. The possibility of the EG$_6$NH$_2$ having accessibility problems due to varied attachment to the gold surface was considered, but since ToF-SIMS typically measures the topmost 1−2 nm of the surface, we strongly believe that the figures of surface composition of EG$_6$NH$_2$ indicate the −NH$_2$ which would be accessible to the peptide when grafting is carried out.

The net charges on the peptide and on the NH$_2$ moieties are both positive in the given grafting conditions, and the stoichiometric ratio of the NH$_2$ to peptide is unfavorable at solution percentages below 10% and above 25% EG$_6$NH$_2$. These contribute to the poor peptide coupling efficiency of these systems. Ethylene glycol units of the longer thiol (EG$_6$NH$_2$) "shield" the molecules beneath it.[20] Thus, at concentrations above 50% EG$_6$NH$_2$ the NH$_2$ termini are spatially closer to each other, and the peptide molecules are unable to access each and every NH$_2$ terminus, giving rise to a lower peptide coupling efficiency. The theoretical surface density of peptide molecules with efficient packing can be calculated using the theoretical diameter of influence as

provided by the space filling model software PYMOL. The theoretical diameter was calculated by PYMOL to be 15 Å, yielding a theoretical surface peptide density for hexagonal close packing on the surface of 0.51 molecules nm^{-2}. However, in this work we observed molecular densities higher than this value when grafting peptide molecules on mixed SAMs. Peptide densities higher than the theoretical value, found at low surface concentrations of NH$_2$, can be explained if the peptides bind (even if to a limited extent) to the surface via −OH groups.[30] We can also attribute this increased density to the availability of NH$_2$ termini on flexible extended "arms" of the EG$_6$NH$_2$ which have three ethylene glycols which are theoretically ∼1 nm (3*length of the theoretical EG unit) extended above the EG$_3$OH base monolayers.

3.4. Specific and Nonspecific Protein Binding Ratio with Peptide Grafted onto Mixed SAM EG$_6$NH$_2$−EG$_3$OH.

The analyte protein, IgG, and the nonspecific protein, BSA, were used to study the specificity of the peptide biosensor system on the mixed SAM and characterize the effects of concentration of monolayers on which the peptides had been grafted. The serum for monoclonal antibody production is often complemented with additives such as those from fetal bovine serum, and BSA has been known to be one of the major protein contaminants in IgG production downstream.[62] Thus, this protein has been used as the reference protein for nonspecific binding onto the peptide-based sensors. The HWRGWV short peptide was grafted onto SPR sensors with mixed monolayers formed from solutions with EG$_6$NH$_2$ concentrations ranging from 5% to 100%. Protein adsorption levels for IgG and BSA solutions (6 mM concentration, each) were recorded, and the ratio of IgG to BSA bound was plotted against the EG$_6$NH$_2$ precursor solution concentration used to build the SAM (Figure 4 (black columns)).
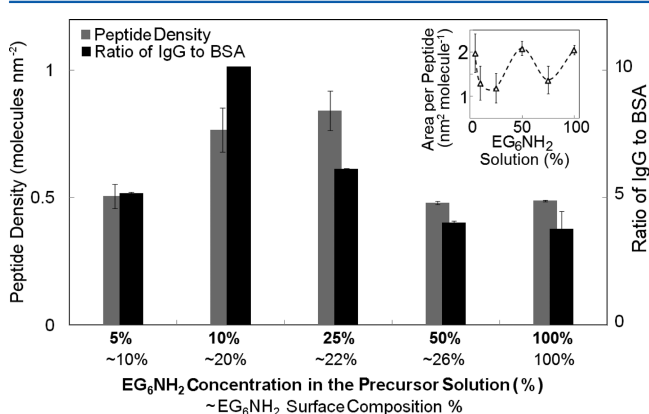

Figure 4. Peptide density (gray) on mixed SAMs and ratio of binding of IgG and BSA (at the same molar concentration) (black) shown for peptides grafted onto monolayers formed from EG$_6$NH$_2$ precursor solutions of the concentration and calculated EG$_6$NH$_2$ surface composition indicated by a "∼" in x-axis. (Inset) Area occupied per peptide molecule for mixed SAMs formed from EG$_6$NH$_2$ precursor solutions of the concentrations shown in the x-axis.

The IgG to BSA ratio reaches maxima at surfaces of prepared 10% EG$_6$NH$_2$ solution. Thus, the mixed monolayer–peptide system prepared from 10% EG$_6$NH$_2$ (with density of 0.77 peptides nm^{-2}) was chosen as ideally suited for biosensor design. For this surface, the area/peptide molecule (calculated as the inverse of peptide density in molecules nm^{-2}, inset Figure 4) showed a local minimum, indicating that the peptide

molecules are optimally spaced. This optimal spatial distribution of peptides surrounded by nonspecific binding detractors (i.e., −OH termini of EG$_3$OH) contributes to the optimum ratio of IgG to BSA molecules bound.

At concentrations of EG$_6$NH$_2$ other than the optimum surface concentration, the inability of the ligands to access all the reactive NH$_2$ groups can lead to a higher percentage of unconverted NH$_2$, leading to higher levels of nonspecific binding due to electrostatic interactions with the available NH$_2$. Authors have found evidence of an enhanced specific binding of optimum ligand attachment, reduced nonspecific binding, or a combination of these on systems with mixed monolayers at intermediate surface concentrations (commonly between 10 and 25% of the reactive species in the monolayers).[63] For example, biotinylated oligo(ethylene glycol) alkanethiol mixed SAMs prepared from 10% precursor solution concentration (∼20% surface composition) showed maximum specifically bound streptavidin in studies by Nelson et al.[19] Another biotinylated alkanethiol mixed SAM system (without OEG units) showed better specific binding toward streptavidin at mixed monolayer concentrations of 57%.

We have already seen in a previous section that the preferential adsorption of EG$_6$NH$_2$ on the SAMs changes after 25% EG$_6$NH$_2$ precursor solution. The peptide density is a maximum at SAMs formed from 25% precursor EG$_6$NH$_2$ solutions and also leads to a higher IgG binding value; however, the specificity of binding (IgG to BSA binding ratio) is higher at 10% EG$_6$NH$_2$. This study has illustrated that using mixed monolayers in conjunction with the active ligands increases the specificity of binding, but the mixed SAMs should be characterized to achieve optimal specificities.

3.5. IgG Binding on Peptides Grafted on Mixed SAMs EG$_6$NH$_2$−EG$_3$OH.

We focus our attention on the peptide systems based on EG$_6$NH$_2$−EG$_3$OH mixed SAMs prepared from 10% EG$_6$NH$_2$ solution (∼20% surface composition). SPR protein binding experiments (IgG and BSA) were carried out on sensors made from peptides grafted onto the mixed SAM. The amount of analyte protein adsorbed to the surface was calculated from the net angle change of sensorgrams before and after analyte injections. The data points were fitted to eq 3 as shown in Figure 5 to yield values of K_d of $9.33 \pm 0.26 \times 10^{-7}$ M and Q_m of 3.177 ± 0.26 mg m^{-2}. The value of K_d was 5.8×10^{-7} M for the same peptide grafted onto the 100% EG$_6$NH$_2$ system; however, the value of Q_m was higher at 3.76 mg m^{-2} on this surface.[64]

Thus, the dilution of the monolayers had no effect on the inherent binding affinity of the ligand toward IgG, but the capacity of the surface was decreased. Even though there is a higher peptide ligand density associated with the mixed monolayer system we observed a lower amount of protein adsorbed, and this is due to the high protein resisting capabilities of the OEG units present in the mixed SAM.

The number of unconverted NH$_2$ termini decreased in the mixed monolayer system leading to a decrease of nonspecific binding of the IgG, as is also demonstrated by the decrease of BSA adsorption on the mixed SAM. We observe in Figure 5 that the maximum BSA adsorption in the presence of the peptides is 0.5 mg m^{-2}, and IgG adsorbed in the absence of peptides (which can also be considered as nonspecific binding) is 0.5 mg m^{-2}. The corresponding values on peptides grafted on SAMs of 100% EG$_6$NH$_2$ were 1 mg m^{-2}.[64]

The implications of these observations are tied to the analyte quality that is to be used. In general the mixed SAMs can be
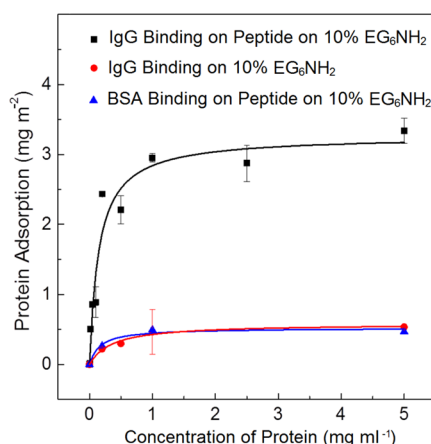
Figure 5. Analysis of protein binding on EG_6NH_2–EG_3OH mixed SAMs with and without peptide grafted. The mixed SAMs were formed from 10% EG_6NH_2 precursor solution (and had ~20% surface composition). Results of IgG adsorption on HWRGWV grafted onto mixed SAM (black), IgG adsorption on mixed SAM with no peptide (red), and BSA adsorption on HWRGWV grafted onto mixed SAM (blue) are shown in the figure.

used in biosensing applications where nonspecific binding must be reduced; i.e., if there is a need for better specificity one should opt for mixed monolayers, and if there is a need for lower levels of detection the pure monolayer system would serve better.

Rate Adsorption Constant. Time-dependent SPR sensorgrams obtained for different IgG (analyte) concentrations were fitted to the kinetic model by solving eqs 6 and 7 to determine the rate adsorption constant k_a. A good fit was obtained for IgG concentrations lower than 1 mg mL^{-1}. At higher IgG

concentrations the change in refractive index is affected by the high protein load, which causes an overshoot that is not accounted for in the kinetic model for IgG–peptide binding. An average k_a of 2.0 ± 0.3 m^3 mol^{-1} s^{-1} was obtained from the fittings (Figure 6(a–f)).

This value corresponded well with our results from IgG binding on peptides grafted onto pure SAM, where average k_a values of 2.2 ± 0.4 and 2.1 ± 0.7 m^3 mol^{-1} s^{-1} were obtained for nonacetylated and acetylated peptides, respectively.[64] We also observed that the experiments are not mass transport limited as seen in Figure 6(g); at time $t \to 0$, the ratio of the concentration of IgG at the surface compared to that in the bulk (C_s/C_b) tends to unity for all concentrations of IgG, indicating that there are no mass transport limitations for the analyte to travel from the bulk of the solution to the biosensing surface.

IgG Detection from Complex Media. For effective use as a biosensor, its performance should be analyzed in complex media. The SPR signals can be used to calculate the response of dilutions of complex mixtures toward the sensor systems. We injected Chinese hamster ovary (CHO) cell supernatant solutions (where the cells were genetically modified to produce human IgG) onto peptides grafted onto SAMs with 100% EG_6NH_2 and 10% EG_6NH_2.

The performance of the peptide sensors toward CHO dilutions with IgG and other impurities (red points in Figure 7(a,b)) conformed well with the performance of the respective sensors toward pure IgG solutions in buffer (black points in Figure 7(a,b)). The theoretical SPR signals for a particular sensor are calculated using the concentration of IgG in the CHO dilution as Q in the Langmuir equation (eq 3) and using previously calculated values of K_d and Q_m. We obtained lower percentage deviations (in the range of ~10−30%) for (i) 100%
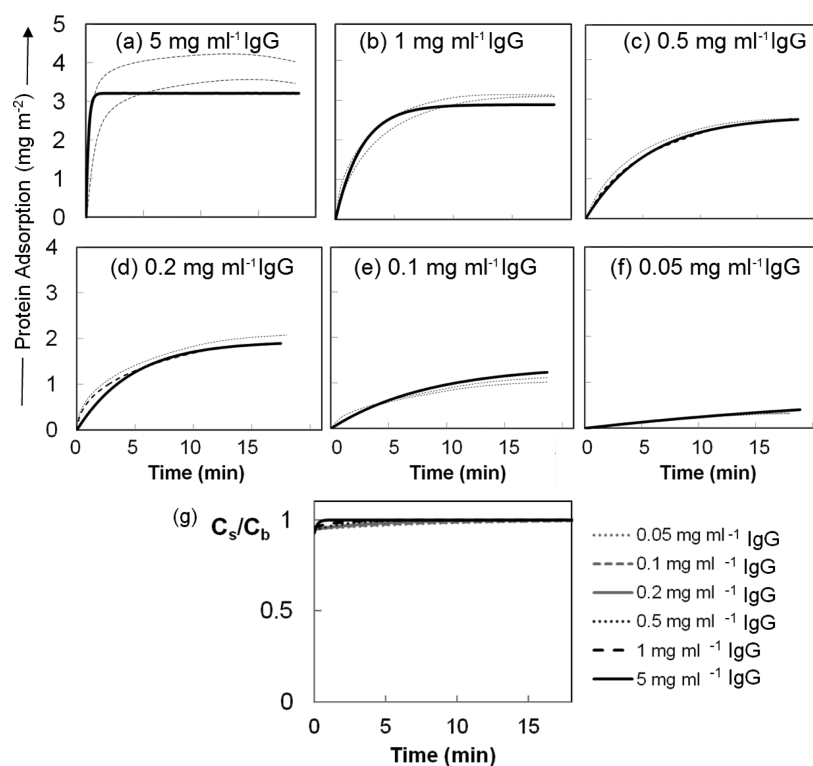

Figure 6. (a−f) SPR fittings of experimental (dotted lines) and theoretical fittings (solid lines) at various concentrations of IgG. (g) C_s/C_b plotted with respect to time at various concentrations of IgG (the legend on the right of the C_s/C_b plot pertains only to this plot).
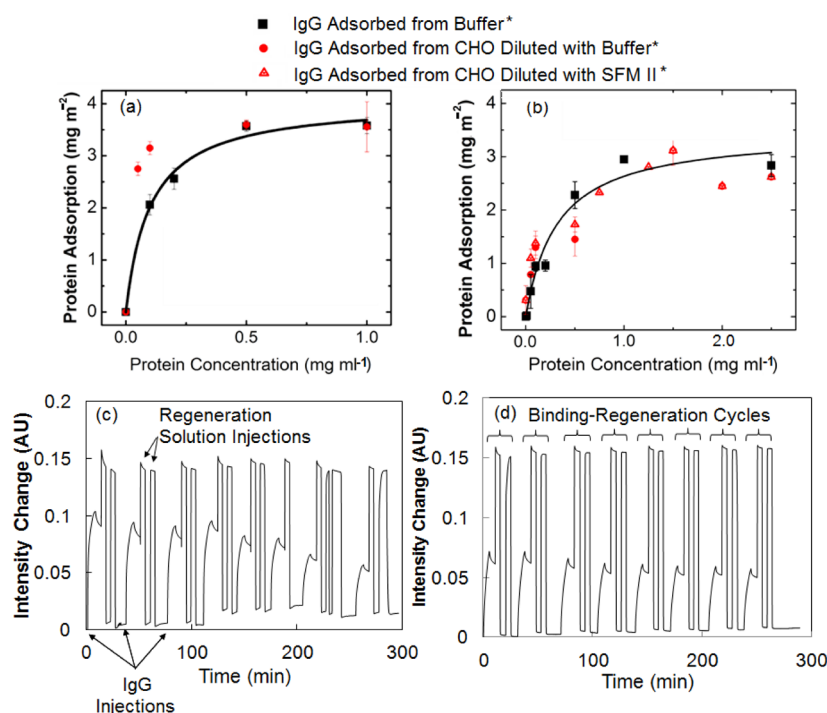
Figure 7. (a) IgG binding from complex mixture dilutions of Chinese hamster ovary (CHO) supernatant on peptides grafted on 100% EG_6NH_2. (b) IgG binding from complex mixture dilutions of CHO supernatant on peptides grafted on mixed SAMs from 10% EG_6NH_2–EG_3OH. (c) IgG binding and regeneration cycles using 0.1 M NaOH + 10% acetonitrile as regeneration solution for a system of peptides grafted on 100% EG_6NH_2. (d) IgG binding and regeneration cycles using 0.1 M NaOH + 10% acetonitrile as regeneration solution for a system of peptides grafted on mixed SAMs from 10% EG_6NH_2–EG_3OH. Also indicated in appropriate arrows and symbols in figures (c) and (d) are IgG injections and regeneration solution injections for different binding–regeneration cycles, and various binding–regeneration cycles are indicated using curly brackets. *Legend above figures pertains to (a) and (b) only.

EG_6NH_2–peptide systems with higher concentrations of a complex mixture (up to 3 times dilutions of CHO) and (ii) for 10% EG_6NH_2–peptide systems when detecting IgG from lower concentrations (from 15 to 300 times CHO dilutions). There was no significant difference observed between the performance on CHO when the diluting media was serum-free media (SFM II, red triangles) and when it was buffer (PBS + 1 N NaCl, red circles). At all concentrations of CHO (with IgG) the capacities and affinity on the 10% EG_6NH_2 were in the same range as that for when binding from PBS solution. These results suggest that the peptide biosensors are viable for IgG detection applications in industrial process streams since CHO cells are frequently employed for commercial production of monoclonal IgG;[65] however, if equilibrium values are used for detection, the response times will be concentration dependent.

We believe that the diluted (mixed) SAMs helped to counter nonspecific binding arising from the contaminants present in the complex mixture. However, at lower dilutions of CHO (i.e., more concentrated mixtures of IgG) there is a possibility that the mixed SAMs displayed bioresistance toward both specific as well as nonspecific binding, which is why mixed SAM-based surfaces would be less suited for concentrated complex mixtures as a detection tool.

Sensor Regeneration. Functional biosensors necessitate the development of effective regeneration conditions. For commercial use of biosensors the system should be suitable for multiple cycles of repeated binding and regeneration, without loss of ligand activity. Optimum regeneration conditions are those which break the bonds between the ligand and analyte without adversely affecting the ligand's binding abilities.

For regeneration of the 100% EG_6NH_2 HWRGWV sensors, we determined the best regeneration solution that caused minimum loss in ligand activity from one of the following regeneration solutions: 0.1 M acetate buffer pH 4.5, 0.1 M NaOH, or 0.1 M NaOH with 10% acetonitrile. Optimum regeneration was obtained for 0.1 M NaOH with 10% acetonitrile, the results of which are shown in Figure 7(c).

Multiple cycles of binding and regeneration were carried out using this solution as is indicated by the curly brackets in Figure 7(d). Detailed analysis shows that there was no loss in activity for the peptide sensors for the first four cycles (binding–regeneration) since the level of IgG adsorbed after each IgG injection (shown in arrows in Figure 7(c)) did not decrease by more than 5%. Conducting four more cycles (for a total of eight cycles) led to a 15% loss in peptide activity and a baseline regeneration of 84% (see Figure 7(c)).

The 0.1 M NaOH with 10% acetonitrile regeneration solution was used for regeneration experiments on 10% EG_6NH_2 HWRGWV sensors. There was negligible loss of peptide activity for the first eight cycles. A 23% loss of peptide activity and a final regeneration baseline of 77% were recorded after 12 cycles. The loss of peptide activity is higher in the case of the mixed monolayers, and this is expected because the NaOH is able to rupture bonds between the –OH and peptides which accounts for ~30% of the peptide bound sites and because the ester bond formed between C termini and OH is susceptible to alkaline conditions.[30] In separate SPR experiments, if the sensors had been pretreated with 0.5 M NaOH (room temperature, 1 h), IgG bound to peptides on mixed SAMs of 10% EG_6NH_2–EG_3OH, but with a decrease in

performance of 25% (data not shown). This can account for the higher loss of activity of peptide grafted on mixed monolayers.

Yang et al. has used mass spectrometry (MS) data and docking simulations to study the nature of bonding between the hexameric peptide HWRGWV and human IgG.[66] They have shown that the most likely binding site is the loop SNGQPENN localized in the C_H3 domain of IgG. They have also pointed out that the binding sites on Protein A or Protein G are different from the peptide binding sites for IgG molecules. These and previous experimental results by the same author[67] indicate that neither hydrophobic nor electrostatic interactions are a dominant force in binding of IgG to the peptide and that hydrogen bonding between residues plays a major role in the specific affinity binding. The results of regeneration experiments carried out in this study are also indicative of the forces prevalent during the binding event of IgG to the ligands. We were unable to regenerate the 100% EG_6NH_2 HWRGWV surface after IgG binding by use of regeneration buffers or solutions such as acetate buffer at pH 4.5 and 0.1 M NaOH with no added acetonitrile. This indicated that merely the change of pH was not enough to cause 100% breaking of bonds between IgG and the peptide. As we see in our results, introduction of a chaotropic agent (e.g., urea) or a polar solvent (e.g., acetonitrile) was required to weaken forces contributed by hydrogen bonding.

4. CONCLUSIONS

The applicability of peptide ligands for detection of human immunoglobulin (IgG) was investigated. Pure and mixed self-assembled monolayers (SAMs) of alkanethiol molecules with oligo(ethylene glycol) units on gold surfaces were implemented to determine the optimum binding of IgG from pure and complex mixtures. Amine-terminated alkanethiols are reactive toward the ligand, and in this work, they were mixed with hydroxyl-terminated alkanethiols which provide antibiofouling properties. Results of surface concentration of mixed SAMs from XPS and ToF-SIMS analyses were in close agreement. In the mixed SAMs of EG_6NH_2–EG_3OH, EG_6NH_2 showed preferential adsorption during coadsorption only up to a certain concentration, which had implications on the subsequent ligand attachment and also on the specificity toward analyte. The surface concentrations and corresponding coverages of NH_2 on mixed SAMs of EG_6NH_2 and EG_3OH were estimated from ToF-SIMS and ellipsometric measurements. The contact angle measurements indicated that the mixed SAMs used to graft ligand HWRGWV were hydrophilic and indicated the potential for reducing the contribution from nonspecific adsorption, as demonstrated in experiments of IgG and BSA binding.

The SPR sensors with peptides grafted onto SAMs from the 10% precursor solution (~20% surface composition) EG_6NH_2 were used for protein binding studies, and the equilibrium and kinetic binding constants were statistically of the same value as those found for peptide grafted on 100% EG_6NH_2. However, the maximum protein adsorbed onto the mixed SAMs with peptides was of lower value as compared to that on the pure SAMs with peptides. The change in the base matrix and in peptide density on the surface did not affect the inherent mechanism of peptide–IgG interaction. Mixing the monolayers did not change the peptide density to a large degree and it also did not affect the IgG–peptide interactions too much. However it did help to minimize nonspecific binding onto the surface which in turn helped to detect IgG with higher precision from

complex mixtures particularly at lower concentrations. The regeneration behavior on peptide on 100% EG_6NH_2 or on 10% EG_6NH_2–EG_3OH was comparable to each other; however, the alkaline regeneration solutions affected performance of the peptide on mixed SAMs. It is thus important to know the precise application of the sensor surface, to help choose the optimum monolayer concentration to develop an effective SPR biosensor.

■ ASSOCIATED CONTENT

ⓈSupporting Information

The details of SPR calibration, calculation of mass transfer coefficient pertaining to SPR flow cell, and the analysis of the kinetic parameters to understand the binding mechanism of IgG can be found in Section S1 and S2. The detailed results of XPS elemental analysis showing the atom percentage for N, S, and O in the EG_3NH_2–EG_3OH mixed SAMs and the plots of N/S and N/O against the EG_3NH_2 concentrations in precursor solution can be found in Section S3. Considerations regarding water coupling are included in Section S4. This material is available free of charge via the Internet at http://pubs.acs.org.

■ AUTHOR INFORMATION

Corresponding Author
*E-mail: ruben@ncsu.edu. Phone: 919-515-5118. Fax: 919-515-3465.

Notes
The authors declare no competing financial interest.

■ REFERENCES

(1) Putzbach, W.; Ronkainen, N. Immobilization Techniques in the Fabrication of Nanomaterial-Based Electrochemical Biosensors: A Review. *Sensors* **2013**, *13*, 4811−4840.

(2) Jans, K.; Bonroy, K.; De Palma, R.; Reekmans, G.; Jans, H.; Laureyn, W.; Smet, M.; Borghs, G.; Maes, G. Stability of Mixed Peo Thiol Sams for Biosensing Applications. *Langmuir* **2008**, *24*, 3949−3954.

(3) Witt, D.; Klajn, R.; Barski, P.; Grzybowski, B. A. Applications, Properties and Synthesis of Omega-Functionalized N-Alkanethiols and Disulfides-the Building Blocks of Self-Assembled Monolayers. *Curr. Org. Chem.* **2004**, *8*, 1763−1797.

(4) Love, J. C.; Estroff, L. A.; Kriebel, J. K.; Nuzzo, R. G.; Whitesides, G. M. Self-Assembled Monolayers of Thiolates on Metals as a Form of Nanotechnology. *Chem. Rev.* **2005**, *105*, 1103−1170.

(5) Huang, L.; Reekmans, G.; Saerens, D.; Friedt, J.-M.; Frederix, F.; Francis, L.; Muyldermans, S.; Campitelli, A.; Hoof, C. V. Prostate-Specific Antigen Immunosensing Based on Mixed Self-Assembled Monolayers, Camel Antibodies and Colloidal Gold Enhanced Sandwich Assays. *Biosens. Bioelectron.* **2005**, *21*, 483−490.

(6) Frederix, F.; Bonroy, K.; Laureyn, W.; Reekmans, G.; Campitelli, A.; Dehaen, W.; Maes, G. Enhanced Performance of an Affinity

5371

dx.doi.org/10.1021/jp411469u | *J. Phys. Chem. C* 2014, 118, 5361−5373

Biosensor Interface Based on Mixed Self-Assembled Monolayers of Thiols on Gold. *Langmuir* **2003**, *19*, 4351−4357.

(7) Uchida, K.; Otsuka, H.; Kaneko, M.; Kataoka, K.; Nagasaki, Y. A Reactive Poly(Ethylene Glycol) Layer to Achieve Specific Surface Plasmon Resonance Sensing with a High S/N Ratio: The Substantial Role of a Short Underbrushed PEG Layer in Minimizing Nonspecific Adsorption. *Anal. Chem.* **2005**, *77*, 1075−1080.

(8) Li, L.; Chen, S.; Zheng, J.; Ratner, B. D.; Jiang, S. Protein Adsorption on Oligo(Ethylene Glycol)-Terminated Alkanethiolate Self-Assembled Monolayers: The Molecular Basis for Nonfouling Behavior. *J. Phys. Chem. B* **2005**, *109*, 2934−2941.

(9) Ostuni, E.; Yan, L.; Whitesides, G. M. The Interaction of Proteins and Cells with Self-Assembled Monolayers of Alkanethiolates on Gold and Silver. *Colloids Surf., B* **1999**, *15*, 3−30.

(10) Scholten, A.; Menges, B.; Juebner, M.; Rothschild, M. A.; Bender, K. A Mixed Alkanethiol Based Immunosensor for Surface Plasmon Field-Enhanced Fluorescence Spectroscopy in Serum. *Analyst* **2013**, *138*, 1705−1712.

(11) Prime, K. L.; Whitesides, G. M. Self-Assembled Organic Monolayers - Model Systems for Studying Adsorption of Proteins at Surfaces. *Science* **1991**, *252*, 1164−1167.

(12) Lahiri, J.; Isaacs, L.; Tien, J.; Whitesides, G. M. A Strategy for the Generation of Surfaces Presenting Ligands for Studies of Binding Based on an Active Ester as a Common Reactive Intermediate: A Surface Plasmon Resonance Study. *Anal. Chem.* **1999**, *71*, 777−790.

(13) Choi, S.; Murphy, W. L. Multifunctional Mixed Sams That Promote Both Cell Adhesion and Noncovalent DNA Immobilization. *Langmuir* **2008**, *24*, 6873−6880.

(14) Nagatomo, K.; Kawaguchi, T.; Miura, N.; Toko, K.; Matsumoto, K. Development of a Sensitive Surface Plasmon Resonance Immunosensor for Detection of 2,4-Dinitrotoluene with a Novel Oligo (Ethylene Glycol)-Based Sensor Surface. *Talanta* **2009**, *79*, 1142−1148.

(15) Bain, C. D.; Whitesides, G. M. Modeling Organic Surfaces with Self-Assembled Monolayers. *Angew. Chem., Int. Ed. Engl.* **1989**, *28*, 506−512.

(16) Choo, H.; Cutler, E.; Shon, Y.-S. Synthesis of Mixed Monolayer-Protected Gold Clusters from Thiol Mixtures: Variation in the Tail Group, Chain Length, and Solvent. *Langmuir* **2003**, *19*, 8555−8559.

(17) Park, J. H.; Park, B. S.; Huh, G.; Lee, S. H.; Lee, H. S.; Cho, I. H.; Paek, S. H.; Lee, H. W. Specific Immobilization of Streptavidin on Mixed Self-Assembled Monolayers as Mixing Ratio. *Solid State Phenom.* **2007**, *121*, 495−498.

(18) Polster, D.; Graaf, H. Advancing and Receding Angles: Dynamic Contact Angle Measurements on Mixed Alkyl Monolayers. *Appl. Surf. Sci.* **2012**, *265*, 88−93.

(19) Nelson, K. E.; Gamble, L.; Jung, L. S.; Boeckl, M. S.; Naeemi, E.; Golledge, S. L.; Sasaki, T.; Castner, D. G.; Campbell, C. T.; Stayton, P. S. Surface Characterization of Mixed Self-Assembled Monolayers Designed for Streptavidin Immobilization. *Langmuir* **2001**, *17*, 2807−2816.

(20) Chapman, R. G.; Ostuni, E.; Yan, L.; Whitesides, G. M. Preparation of Mixed Self-Assembled Monolayers (Sams) That Resist Adsorption of Proteins Using the Reaction of Amines with a Sam That Presents Interchain Carboxylic Anhydride Groups. *Langmuir* **2000**, *16*, 6927−6936.

(21) Zorn, S.; Dettinger, U.; Skoda, M. W. A.; Jacobs, R. M. J.; Peisert, H.; Gerlach, A.; Chassé, T.; Schreiber, F. Stability of Hexa(Ethylene Glycol) Sams Towards the Exposure to Natural Light and Repeated Reimmersion. *Appl. Surf. Sci.* **2010**, *258*, 7882−7888.

(22) Shuster, M. J.; Vaish, A.; Gilbert, M. L.; Martinez-Rivera, M.; Nezarati, R. M.; Weiss, P. S.; Andrews, A. M. Comparison of Oligo(Ethylene Glycol)Alkanethiols Versus N-Alkanethiols: Self-Assembly, Insertion, and Functionalization. *J. Phys. Chem. C* **2011**, *115*, 24778−24787.

(23) Lin, Y.-C.; Yu, B.-Y.; Lin, W.-C.; Lee, S.-H.; Kuo, C.-H.; Shyue, J.-J. Tailoring the Surface Potential of Gold Nanoparticles with Self-

Assembled Monolayers with Mixed Functional Groups. *J. Colloid Interface Sci.* **2009**, *340*, 126−130.

(24) Chirakul, P.; Pérez-Luna, V. H.; Owen, H.; López, G. P.; Hampton, P. D. Synthesis and Characterization of Amine-Terminated Self-Assembled Monolayers Containing Diethylene Glycol Linkages. *Langmuir* **2002**, *18*, 4324−4330.

(25) Jung, L. S.; Campbell, C. T.; Chinowsky, T. M.; Mar, M. N.; Yee, S. S. Quantitative Interpretation of the Response of Surface Plasmon Resonance Sensors to Adsorbed Films. *Langmuir* **1998**, *14*, 5636−5648.

(26) Cheng, F.; Gamble, L. J.; Castner, D. G. XPS, Tof-Sims, NEXAFS, and SPR Characterization of Nitrilotriacetic Acid-Terminated Self-Assembled Monolayers for Controllable Immobilization of Proteins. *Anal. Chem.* **2008**, *80*, 2564−2573.

(27) Bae, Y. M.; Oh, B.-K.; Lee, W.; Lee, W. H.; Choi, J.-W. Study on Orientation of Immunoglobulin G on Protein G Layer. *Biosens. Bioelectron.* **2005**, *21*, 103−110.

(28) Pavan, S.; Berti, F. Short Peptides as Biosensor Transducers. *Anal. Bioanal. Chem.* **2010**, *402*, 3055−3070.

(29) Yang, H.; Gurgel, P. V.; Carbonell, R. G. Hexamer Peptide Affinity Resins That Bind the Fc Region of Human Immunoglobulin G. *J. Pept. Res.* **2005**, *66*, 120−137.

(30) Menegatti, S.; Naik, A. D.; Gurgel, P. V.; Carbonell, R. G. Alkaline-Stable Peptide Ligand Affinity Adsorbents for the Purification of Biomolecules. *J. Chromatogr. A* **2010**, *1245*, 55−64.

(31) Naik, A. D.; Menegatti, S.; Gurgel, P. V.; Carbonell, R. G. Performance of Hexamer Peptide Ligands for Affinity Purification of Immunoglobulin G from Commercial Cell Culture Media. *J. Chromatogr. A* **2011**, *1218*, 1691−1700.

(32) Zhang, Y.; Islam, N.; Carbonell, R. G.; Rojas, O. J. Specific Binding of IgG with Bioactive Short Peptides Supported on Antifouling Copolymer Layers for Detection in QCM and SPR. *Anal. Chem.* **2012**, *85*, 1106−1113.

(33) Yu, Q.; Chen, S.; Taylor, A. D.; Homola, J.; Hock, B.; Jiang, S. Detection of Low-Molecular-Weight Domoic Acid Using Surface Plasmon Resonance Sensor. *Sens. Actuators, B* **2005**, *107*, 193−201.

(34) Wang, H.; Chen, S.; Li, L.; Jiang, S. Improved Method for the Preparation of Carboxylic Acid and Amine Terminated Self-Assembled Monolayers of Alkanethiolates. *Langmuir* **2005**, *21*, 2633−2636.

(35) Johansson, L.-S.; Campbell, J. M. Reproducible XPS on Biopolymers: Cellulose Studies. *Surf. Interface Anal.* **2004**, *36*, 1018−1022.

(36) Cooper, E.; Leggett, G. J. Static Secondary Ion Mass Spectrometry Studies of Self-Assembled Monolayers: Influence of Adsorbate Chain Length and Terminal Functional Group on Rates of Photooxidation of Alkanethiols on Gold. *Langmuir* **1998**, *14*, 4795−4801.

(37) Pan, S.; Castner, D. G.; Ratner, B. D. Multitechnique Surface Characterization of Derivatization Efficiencies for Hydroxyl-Terminated Self-Assembled Monolayers. *Langmuir* **1998**, *14*, 3545−3550.

(38) Offord, D. A.; John, C. M.; Griffin, J. H. Contact Angle Goniometry, Ellipsometry, XPS, and Tof-Sims Analysis of Gold-Supported, Mixed Self-Assembled Monolayers Formed from Mixed Dialkyl Disulfides. *Langmuir* **1994**, *10*, 761−766.

(39) Wolf, K. V.; Cole, D. A.; Bernasek, S. L. Chain Length Effects for Cluster Ion Formation During High Energy Ion/Surface Collisions with Self-Assembled Monolayer Surfaces. *J. Phys. Chem. B* **2002**, *106*, 10382−10387.

(40) Baugh, L.; Weidner, T.; Baio, J. E.; Nguyen, P.-C. T.; Gamble, L. J.; Stayton, P. S.; Castner, D. G. Probing the Orientation of Surface-Immobilized Protein G B1 Using ToF-SIMS, Sum Frequency Generation, and NEXAFS Spectroscopy. *Langmuir* **2010**, *26*, 16434−16441.

(41) Cheng, F.; Gamble, L. J.; Grainger, D. W.; Castner, D. G. X-Ray Photoelectron Spectroscopy, Time-of-Flight Secondary Ion Mass Spectrometry, and Principal Component Analysis of the Hydrolysis, Regeneration, and Reactivity of N-Hydroxysuccinimide-Containing Organic Thin Films. *Anal. Chem.* **2007**, *79*, 8781−8788.

(42) Arwin, H. Is Ellipsometry Suitable for Sensor Applications? *Sens. Actuators A: Phys.* **2001**, *92*, 43−51.

(43) Karlsson, R.; Michaelsson, A.; Mattsson, L. Kinetic Analysis of Monoclonal Antibody-Antigen Interactions with a New Biosensor Based Analytical System. *J. Immunol. Methods* **1991**, *145*, 229−240.

(44) Wirde, M.; Gelius, U.; Nyholm, L. Self-Assembled Monolayers of Cystamine and Cysteamine on Gold Studied by XPS and Voltammetry. *Langmuir* **1999**, *15*, 6370−6378.

(45) Mrksich, M. Mass Spectrometry of Self-Assembled Monolayers: A New Tool for Molecular Surface Science. *ACS Nano* **2008**, *2*, 7−18.

(46) Tosatti, S.; Michel, R.; Textor, M.; Spencer, N. D. Self-Assembled Monolayers of Dodecyl and Hydroxy-Dodecyl Phosphates on Both Smooth and Rough Titanium and Titanium Oxide Surfaces. *Langmuir* **2002**, *18*, 3537−3548.

(47) Folkers, J. P.; Laibinis, P. E.; Whitesides, G. M. Self-Assembled Monolayers of Alkanethiols on Gold: Comparisons of Monolayers Containing Mixtures of Short- and Long-Chain Constituents with Methyl and Hydroxymethyl Terminal Groups. *Langmuir* **1992**, *8*, 1330−1341.

(48) Park, H. H.; Ivanisevic, A. Formation and Characterization of Homogeneous and Mixed Self-Assembled Monolayers of Peptides and Alkanethiols on Indium Phosphide Surfaces. *J. Phys. Chem. C* **2007**, *111*, 3710−3718.

(49) Riepl, M.; Enander, K.; Liedberg, B.; Schäferling, M.; Kruschina, M.; Ortigao, F. Functionalized Surfaces of Mixed Alkanethiols on Gold as a Platform for Oligonucleotide Microarrays. *Langmuir* **2002**, *18*, 7016−7023.

(50) Mehne, J.; Markovic, G.; Pröll, F.; Schweizer, N.; Zorn, S.; Schreiber, F.; Gauglitz, G. n. Characterisation of Morphology of Self-Assembled PEG Monolayers: A Comparison of Mixed and Pure Coatings Optimised for Biosensor Applications. *Anal. Bioanal. Chem.* **2008**, *391*, 1783−1791.

(51) Bain, C. D.; Evall, J.; Whitesides, G. M. Formation of Monolayers by the Coadsorption of Thiols on Gold: Variation in the Head Group, Tail Group, and Solvent. *J. Am. Chem. Soc.* **1989**, *111*, 7155−7164.

(52) Kang, J. F.; Liao, S.; Jordan, R.; Ulman, A. Mixed Self-Assembled Monolayers of Rigid Biphenyl Thiols: Impact of Solvent and Dipole Moment. *J. Am. Chem. Soc.* **1998**, *120*, 9662−9667.

(53) Arima, Y.; Iwata, H. Effect of Wettability and Surface Functional Groups on Protein Adsorption and Cell Adhesion Using Well-Defined Mixed Self-Assembled Monolayers. *Biomaterials* **2007**, *28*, 3074−3082.

(54) Faucheux, N.; Schweiss, R.; Lützow, K.; Werner, C.; Groth, T. Self-Assembled Monolayers with Different Terminating Groups as Model Substrates for Cell Adhesion Studies. *Biomaterials* **2004**, *25*, 2721−2730.

(55) Extrand, C. W. Contact Angles and Hysteresis on Surfaces with Chemically Heterogeneous Islands. *Langmuir* **2003**, *19*, 3793−3796.

(56) Pale-Grosdemange, C.; Simon, E. S.; Prime, K. L.; Whitesides, G. M. Formation of Self-Assembled Monolayers by Chemisorption of Derivatives of Oligo (Ethylene Glycol) of Structure $HS(CH_2)11-(OCH_2CH_2)_mOH$ on Gold. *J. Am. Chem. Soc.* **1991**, *113*, 12−20.

(57) Wink, T.; vanZuilen, S. J.; Bult, A.; vanBennekom, W. P. Self-Assembled Monolayers for Biosensors. *Analyst* **1997**, *122*, R43−R50.

(58) Briand, E.; Salmain, M.; Compère, C.; Pradier, C.-M. Immobilization of Protein A on Sams for the Elaboration of Immunosensors. *Colloids Surf., B* **2006**, *53*, 215−224.

(59) Wang, D. S.; Chang, C. C.; Shih, S. C.; Lin, C. W. An Ellipsometric Study on the Density and Functionality of Antibody Layers Immobilized by a Randomly Covalent Method and a Protein A-Oriented Method. *Biomed. Eng.-Appl. Basis Commun.* **2009**, *21*, 303−310.

(60) Unsworth, L. D.; Sheardown, H.; Brash, J. L. Protein Resistance of Surfaces Prepared by Sorption of End-Thiolated Poly(Ethylene Glycol) to Gold: Effect of Surface Chain Density. *Langmuir* **2005**, *21*, 1036−1041.

(61) Zhu, B.; Eurell, T.; Gunawan, R.; Leckband, D. Chain-Length Dependence of the Protein and Cell Resistance of Oligo(Ethylene Glycol)-Terminated Self-Assembled Monolayers on Gold. *J. Biomed. Mater. Res.* **2001**, *56*, 406−416.

(62) Berry, J. D. Rational Monoclonal Antibody Development to Emerging Pathogens, Biothreat Agents and Agents of Foreign Animal Disease: The Antigen Scale. *Vet. J.* **2005**, *170*, 193−211.

(63) Spinke, J.; Liley, M.; Schmitt, F. J.; Guder, H. J.; Angermaier, L.; Knoll, W. Molecular Recognition at Self-Assembled Monolayers: Optimization of Surface Functionalization. *J. Chem. Phys.* **1993**, *99*, 7012−7019.

(64) Islam, N. Surface Plasmon Resonance Studies of the Specific Interactions of Hexamer Peptide Ligands with Human Immunoglobulin G, *Phd Thesis*, North Carolina State University, Raleigh, NC, 2013.

(65) Kim, J. Y.; Kim, Y.-G.; Lee, G. M. Cho Cells in Biotechnology for Production of Recombinant Proteins: Current State and Further Potential. *Appl. Microbiol. Biotechnol.* **2012**, *93*, 917−930.

(66) Yang, H. O.; Gurgel, P. V.; Williams, D. K.; Bobay, B. G.; Cavanagh, J.; Muddiman, D. C.; Carbonell, R. G. Binding Site on Human Immunoglobulin G for the Affinity Ligand HWRGWV. *J. Mol. Recognit.* **2010**, *23*, 271−282.

(67) Yang, H.; Gurgel, P. V.; Carbonell, R. G. Purification of Human Immunoglobulin G Via Fc-Specific Small Peptide Ligand Affinity Chromatography. *J. Chromatogr. A* **2009**, *1216*, 910−918.

5373

dx.doi.org/10.1021/jp411469u | *J. Phys. Chem. C* 2014, 118, 5361−5373